*Graphical Abstract

Variability of global mean annual temperature is significantly influenced by the rhythm of ocean-atmosphere oscillations

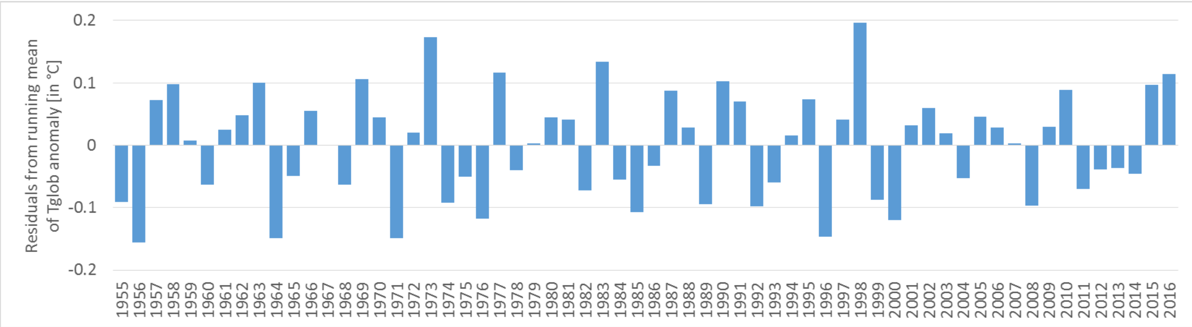

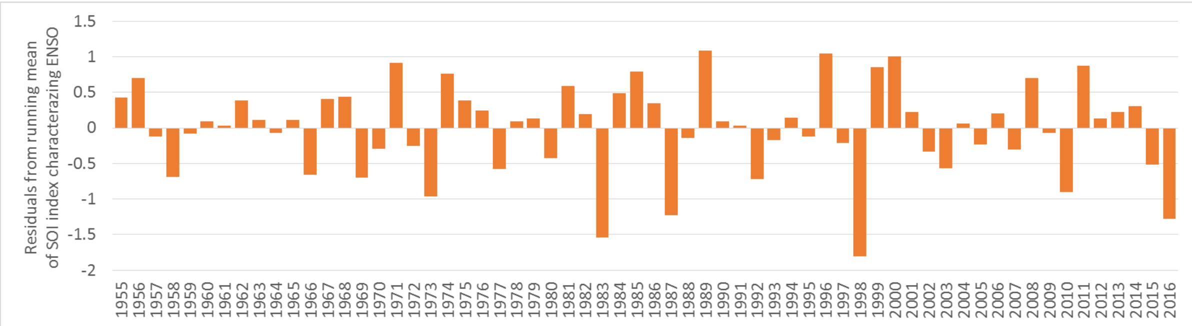

*Highlights (for review : 3 to 5 bullet points (maximum 85 characters including spaces per bullet point)

Variability of global mean annual temperature is significantly influenced by the rhythm of ocean-atmosphere oscillations

The rhythm of ocean-atmosphere oscillation influences global temperature.

Atmosphere-ocean interplay explains deviations of global temperature from trend.

Correlation with ENSO and AMO indices explains 70% of global temperature variability.

Variability of global mean annual temperature is significantly influenced by the rhythm of ocean-atmosphere oscillations

Zbigniew W. Kundzewicz[1], Iwona Pińskwar[1] & Demetris Koutsoyiannis[2]

[1]Institute for Agricultural and Forest Environment, Polish Academy of Sciences, Poznań, Poland, Bukowska 19, 60-809

[2]Department of Water Resources and Environmental Engineering, School of Civil Engineering, National Technical University of Athens, Zographou, Greece

Iwona Pińskwar – corresponding author

E-mail: iwona.pinskwar@isrl.poznan.pl

Abstract

While global warming has been evolving over several decades, in particular years there have been considerable deviations of global temperature from the underlying trend. These could be explained by climate variability patterns and, in particular, by the major interplays of atmospheric and oceanic processes that generate variations in the global climatic system. Here we show, in a simple and straightforward way, that a rhythm of the major ocean-atmosphere oscillations, such as the ENSO and IPO in the Pacific as well as the AMO in the Atlantic, is indeed meaningfully influencing the global mean annual temperature. We construct time series of residuals of the global temperature from the medium-term (5-year) running averages and show that these largely follow the rhythm of residuals of three basic ocean-atmosphere oscillation modes (ENSO, IPO and AMO) from the 5-year running averages. We find

meaningful correlations between analyzed climate variability and deviations of global mean annual temperature residuals that are robust across various datasets and assumptions and explain over 70% of the annual temperature variability in terms of residuals from medium-term averages.

Key words

Global temperature; climate variability, ENSO, IPO, AMO, SSN, VEI

1. Introduction

Essential factors driving the energy balance of the Earth and its mean surface temperature include: the solar radiation, properties of the atmosphere (content of greenhouse gases, dust and aerosols resulting from volcanic eruptions as well as natural and anthropogenic processes) and characteristics of the Earth's surface, such as albedo (Trenberth et al., 2009). In addition, there are several patterns of unforced internal fluctuations in the ocean-atmosphere system that influence the climate (e.g. Mann et al., 2014; Mann and Park, 1994; Tsonis et al., 2005: Power et al., 1999; England et al., 2014; Henley & King, 2017 and many other studies).

Increasing trend of mean global annual temperature has been noted over several decades, which IPCC (2013) has assessed as being extremely likely driven by anthropogenic activities. The most essential IPCC's attribution statements have been getting stronger and stronger, from the first to the fifth IPCC assessment reports. Specifically, in the first two reports IPCC saw "little evidence" (IPCC, 1990), and then "discernible human influence" (IPCC, 1995). In the third, fourth and fifth report, the association of most of the recent warming and anthropogenic greenhouse gas concentration was assessed as likely (subjective probability in excess of 66%), very likely (greater than 90%) and extremely likely (over 95%) in (IPCC, 2001, 2007 and 2013), respectively.

Stanisławska et al. (2012, 2013) used evolutionary computation to hindcast global temperature based on a set of climate drivers and concluded that atmospheric concentration of greenhouse gases is a necessary ingredient of the modelling process, allowing reconstruction of the increasing temperature.

Yet, in a particular year, there can be strong deviations from the warming trend of recorded global temperature that could be explained by climate variability patterns and, in particular, the major interplays of atmospheric and oceanic processes that generate variations in the global climatic system (e.g. Mann et al., 2014; Mann and Park, 1994; Tsonis et al., 2005).

We aim to investigate clear and easily identified links between residuals (deviations from medium-term, namely 5-year, running averages) of global temperature and climate variability indices. We show that the rhythm of major ocean-atmosphere oscillations (climate variability), such as the ENSO and IPO in the Pacific and the AMO in the Atlantic, is indeed influencing the global mean annual temperature.

2. Data and methods

2.1. Global mean temperature

Global mean temperature "anomalies" (i.e. deviations from a long-term average for a reference period) are determined, on a regular basis, by several institutions in the UK, the USA and other countries. Table S1 in the Supplementary Material presents information on three time series of global mean temperature anomalies (land and ocean) used in this paper, stemming from the Climatic Research Unit (CRU) of the University of East Anglia, as well as two agencies in the USA: National Oceanic and Atmospheric Administration (NOAA) and National Aeronautics and Space Administration (NASA). Table S1 contains information on the data owner and UPL address of the record, interval of data availability (being 1850-2019 for HadCRUT4 record of CRU and 1880-2019 for NOAA and NASA series), time step (monthly for CRU and annual for the other two records), as well as the reference periods.

Different data records differ in several ways, including station coverage and reference intervals. The records are updated, reprocessed and enriched on a regular basis (cf. Brohan et al., 2006; Rayner et al., 2006; Harris et al., 2014).

2.2. Climate variability indices

Many climate variability indices have been proposed by different authors and used in their studies (see reviews in Kundzewicz et al., 2019b and Norel et al., 2020).

The *El Niño*–Southern Oscillation (ENSO), associated with irregular, quasi-periodic (or else anti-persistent), variation of sea surface temperature (SST) and air pressure over the tropical Pacific Ocean is broadly recognized as the principal climate variability mode (Mc Phaden et al., 2006). However, there exists a plethora of various indices related to ENSO – a class of Niño indices and SOI (Southern Oscillation Index) that have been used by various authors (see Kaplan, 2011). Information on 12 different indices, summarized in Table S2, refers to data availability, reference period, and the URL address of the source. Many ENSO indices are similar (correlated or anti-correlated, for instance various Niño indices are correlated, while SOI indices are typically anti-correlated to Niño indices). All ENSO data used in this paper are available as monthly mean values, except for NOAA's Oceanic Niño Index (ONI), where 3-month running mean values are used.

The Interdecadal Pacific Oscillation (IPO) is another manifestation of the climate variability in the ocean-atmosphere system involving the Pacific Ocean. We use an IPO Tripole Index (TPI), associated with a distinct 'tripole' pattern of SST anomalies, based on the difference between the SST anomalies averaged over the Central Equatorial Pacific, the Northwest and Southwest Pacific (Henley et al., 2015).

Yet another important mode of large-scale climate variability is the multi-decadal climate oscillation in the Atlantic (see Folland et al., 1984; Schlesinger and Ramankutty, 1994, 1995; and Kerr, 2000). We used the monthly values of the Atlantic Meridional Oscillation (another name: Atlantic Multi-decadal Oscillation) index, i.e. the AMO index retrieved from https://www.esrl.noaa.gov/psd/data/correlation//amon.us.long.data.

We also considered two other natural sources of climate variability, that is the solar activity and the volcanic eruptions. We retrieved the data on sunspot indices, SSN, from WDC-SILSO, Royal Observatory of Belgium, http://sidc.oma.be/silso/datafiles and data on Volcanic Eruptivity Index, VEI, from the portal https://www.ngdc.noaa.gov/hazard/volcano.shtml.

2.3. Exploratory data analysis

We used simple and robust tools that lend themselves well to the situation in hand. We first examined the global mean annual temperature records from three sources by considering 12 shifted time intervals of 30-year length each, starting in 1880, each commencing with a 10-year time step, i.e. 1880-1909, 1890-1919, …,, 1980-2009 and 1990-2019, as well as the total interval of 140 years, 1880-2019, common to all three datasets. We used linear regression for shifted 30-year intervals and for the complete period of 140 years.

Each time series of estimates of global annual temperature consists of 140 numbers. We also analyzed shifted 30-year windows. Here, the size of 30 numbers is at the verge of a condition of a small sample in statistics. Yet, this approach makes it possible to demonstrate changes.

In order to achieve good fit to the temperature data, while keeping simplicity, we used the annual time series from the medium-term (5-year) running averages of global temperature anomalies for the time interval 1880-2019.

We examined residuals, i.e. deviations of temperature values in an individual year from the running averages and we searched for links of these with time series of residuals of climate variability indices from the medium-term (5-year) running averages (based on monthly data).

In brief, our approach follows the spirit of exploratory data analysis. We let the data speak for themselves by looking carefully at the raw numbers. We tried to read the pattern that is present in the records and search for links that can be unveiled by simple tools.

3. Results

3.1. Increase of global mean temperature

The fact that global mean temperature has been dynamically increasing is commonly known, despite some skepticism or controversy about the causes, natural or anthropogenic (Kundzewicz et al., 2019a, 2020). Figure S1 illustrates three time series of annual global mean temperature anomalies stemming from different sources (NASA; NOAA; CRU). Table 1 shows the rates of change (corresponding to linear regression) of annual global temperature for shifted 30-year intervals and for the whole examined interval (1880-2019), common for three time series. It also shows the values of the coefficient of determination (R^2) between the time [in years] and the time series of temperature anomalies, which, as expected, increases with increasing (positive or negative) trend.

Up to 1950-1979 the trends have been alternating between positive and negative. Later the trends have been consistently positive. If we assess the increasing trends of the 30-year periods, i.e. 1950-1979, 1960-1989, 1970-1999, 1980-2009, and 1990-2019, by classical statistics, in which annual values are regarded as independent samples, then these trends turn out to be statistically significant (at the 0.05 level); also statistically significant turns out to be the decreasing trend over 1880-1909. However, in can be readily seen that there is no independence among the annual values, while it has been shown that neglecting dependence substantially overestimates the statistical significance and downplays uncertainty (Koutsoyiannis, 2003; Cohn and Lins, 2005; Koutsoyiannis and Montanari, 2007; Hamed, 2008). For this reason, we avoid associating our findings with statistical significance and we prefer to focus on the rate of temperature increase. During the last 30-year period, 1990-2019, this latter has been much higher than in any earlier interval and amounts to between 1.78 and 2.10 °C per 100 years, where these two values correspond to the data of CRU and NASA, respectively. As seen in Table 1, over the entire period of records, the trend values vary between 0.68 °C per 100 years for the CRU data set to 0.74 °C per 100 years for the NASA and NOAA data sets.

Next, we calculated deviations of temperature anomaly in any given year from the annual time series from the medium-term (5-year) running averages of global temperature - anomalies for the time interval 1880-2019. They are illustrated in Fig. S2.

3.2. Climate variability indices *vs* global temperature

3.2.1. ENSO indices

Some authors demonstrated evidence of a link between the *El Niño*–Southern Oscillation (ENSO) and large-scale temperature (Yulaeva and Wallace, 1994; Tourre and White, 1995; Tsonis et al., 2005; Thompson et al., 2009). We look into these links for updated records from three sources, reaching to 2019. Many ENSO (or SOI) types of indices have been used in literature, hence, we examine a set of them in our search for a link with global temperature.

Careful optical comparison of time series illustrated in Figs 1a and 1b makes it possible to conclude that often the signs of residuals from 5-year running mean of temperature (CRU) and of Equatorial SOI index characterizing ENSO are in counterphase for an individual year (there is a positive residual for one series and a negative for another one). However, the amplitude can largely differ – there can be a small value of one series and a large one for another one in a particular year.

The Niño indices have longer temporal coverage than the Equatorial SOI index, as the data start at 1879. Time series of residuals from 5-year running mean of temperature (NASA) and of Niño 3 index are illustrated in Fig. 2. The signs of both series of residuals are often in phase for an individual year, yet the amplitude can differ.

Table 2 presents values of the coefficient of determination (R^2) between time series of residuals from 5-year running mean of temperature anomalies (land and ocean) and residuals from 5-year running mean of various ENSO indices. The values of R^2 are fairly high. Except for EMI, the values for all 11 ENSO indices and for all three time series of global temperature are between 0.400 and 0.590. Optimal selection of the starting month of the 12-month moving average of various ENSO indices warrants highest value of the coefficient of determination. Justification for trying different starting months is provided by the fact that, if seen at the monthly time scale, there appears to be a time lag of a few months between ENSO and its effect on global temperature. To capture this lag on the annual scale we need to modify the starting (and ending) month of a year.

For the CRU temperature deviations the highest value of R^2 (0.590) was noted for Equatorial SOI index, for NOAA temperature data – for Equatorial SOI Indonesia index (0.575) and for NASA data – for Niño 3 index (0.509). Selection of the optimal starting month of the 12-month moving average of various ENSO indices is illustrated in Table S3 for an example of residuals from 5-year running mean of various ENSO indices: Equatorial SOI Indonesia and Niño 3 index and residuals from 5-year running mean of temperature anomalies (land and ocean) (after CRU and NASA). Even if the R^2 values for July-June and August-July are the highest, nearly all 12 selections lead to reasonably strong links.

3.2.2. IPO

There are literature hints that the Interdecadal Pacific Oscillation (IPO) can be associated with variability in large-scale temperature (England et al., 2014; Henley & King, 2017).

We searched for links between residuals from 5-year running mean values of the IPO TPI index and those of the global annual mean temperature (land and ocean).

The values of the coefficient of determination (R^2) for "best" selection of 12-month moving average of residuals from 5-year running mean of the IPO TPI index (September-August) and residuals from 5-year running mean of global temperature anomalies (land and ocean) are: 0.493 for NOAA, 0.469 for CRU and 0.454 for NASA.

3.2.3. AMO

Some authors demonstrated evidence of a link between the Atlantic Meridional Oscillation (another name: Atlantic Multi-decadal Oscillation) index, i.e. the AMO index and large-scale temperature (van der Werf and Dolman, 2014, Nagy et al., 2017, Frajka-Williams et al., 2017). We searched for links between residuals from 5-year running mean values of the AMO index and those of the global annual mean temperature (land and ocean) for 1882-2016 (Fig. 3). We used all three sources of temperature data (NASA; NOAA, CRU). Comparing Fig. 3a,b,c and Fig. 3d we can conclude that often the sign of residuals of global mean temperature (from each of the three sources, in Figs 3a,b,c) and the sign of the residuals of the AMO index (Fig. 3d) are the same for an individual year. However, the amplitude of residuals of temperature and of the AMO index can largely differ.

The values of the coefficient of determination (R^2) for "best" selection of 12-month moving average of residuals from 5-year running mean of the AMO index and of global temperature anomalies (land and ocean) for 1882-2016, are: 0.418 for NOAA, 0.389 for CRU and 0.373 for NASA.

3.2.4. Joint consideration of climate variability indices

As shown in sections 3.2.1, 3.2.2 and 3.2.3, links have been found between time series of residuals from 5-year running mean of temperature and of particular ENSO indices as well as of temperature and of IPO and AMO indices. Therefore, joint consideration of pairs of climate variability indices was undertaken. Results presented in Table 3 demonstrate that the value of coefficient of determination are higher than when considering only one oscillation pattern, ENSO or AMO. Since various ENSO indices are available, we considered 12 of them in calculations, noting high R^2 values for all ENSO indices, ranging from 0.454 to 0.698.

For temperature data from different sources, the highest values of R^2 were noted for SOI NOAA index, equal to 0.698, 0.697 and 0.607, for CRU, NOAA and NASA, respectively. These results indicate that, with appropriate selection of indices and with reference to medium-term temperature fluctuation, a large proportion, nearly 70%, of the annual variability of the latter is explained by the ENSO and AMO evolution.

Joint consideration of ENSO and IPO TPI links with temperature, for 11 ENSO indices (EMI excluded) gave R^2 values ranging from 0.454 to 0.612 (Table S4). Likewise, joint consideration of IPO TPI and AMO links with temperature gave R^2 values at the level of 0.632 for NOAA, 0.590 for CRU and 0.575 for NASA.

Finally, joint consideration of a triplet: ENSO, IPO TPI, and AMO, with temperature gave R^2 values at the level up to 0.707 for NOAA, 0.706 for CRU and 0.614 for NASA (Table S5). Hence, more than 70% of the medium-term annual variability of temperature is explained by the ENSO, IPO TPI, and AMO evolution.

Guided by the principle of parsimony (Occam's razor) it may be questioned whether three explanatory variables (ENSO, IPO TPI, and AMO) are preferred over two (ENSO and AMO), once the third variable did not result in a major improvement of the value of R^2 (0.707 as opposed to 0.698).

3.2.5. Sunspot and volcanic track

For completeness, we also examined the strength of links of 5-year running mean of temperature anomalies and the characteristics of two other mechanisms of climate variability - the activity of the Sun, the principal driver of Earth´s climate and the volcanic eruptions. The former was expressed by sunspot numbers (SSNs), while the latter – by the Volcanic Eruptivity Index, VEI (see Newhall and Self, 1982 and Mason et al., 2004). For correlation, annual sums of sunspot numbers were used, while the values of VEI from 4 to 6 were transformed to volume according to Newhall and Self (1982) (see also https://www.ngdc.noaa.gov/nndc/DescribeField.jsp?dataset=102557&s=77&field_name=HAZ.VOLCANO_EVENT.VEI) and monthly sums were used as annual values. We found that R^2 values for both annual SSN and VEI were very low: from 0.01 to 0.02 for annual sum for previous year for SSN and for 0.009 to 0.004 for annual sum of volcanic volume for the same year. Joint consideration of SSN and VEI also did not dramatically improve the value of R^2 (from 0.02 to 0.03).

Interesting interplay of volcanic eruption and ocean-atmosphere oscillation can be illustrated at an example of the year 1992, when the global temperature residual was negative and quite strong, while the value of the ONI NOAA FMA index was positive and high, and that of AMO was slightly negative. Drop of global temperature despite a warm El Niño phase can be interpreted as a possible climatic effect of eruption of the Pinatubo Volcano on 15 June 1991. However, this interplay is not captured by linear statistical models as indicated by the low R^2 of linear regression.

4. Concluding remarks

It is commonly recognized that global warming has been unabated over several decades. However, in individual years there are strong deviations of global temperature from the underlying tendency that could be explained by climate variability patterns. Essential can be the major interplays of atmospheric and oceanic processes that generate variations in the global climatic system.

In this paper, we attempted to demonstrate, in a straightforward yet persuading way, that a rhythm of the major ocean-atmosphere oscillations (climate variability), such as the

ENSO and IPO in the Pacific and the AMO in the Atlantic, is indeed influencing the global mean annual temperature. We found links between time series of residuals from 5-year running mean of temperature (land and ocean) and of particular ENSO indices. The R^2 values are fairly high. Except for EMI, the values for all remaining 11 ENSO indices and for all three time series of global temperature ranged from 0.400 to 0.590.

We also found links between time series of residuals from 5-year running mean of temperature and of IPO TPI or AMO indices, with R^2 values for various temperature data sources ranging from 0.454 to 0.493 for IPO TPI and from 0.373 to 0.418 for AMO.

Therefore joint consideration of links between time series of residuals from 5-year running mean of temperature and various pairs of the three: ENSO, IPO TPI, and AMO indices was undertaken and the R^2 values were found to be higher than when considering only one oscillation pattern. For ENSO and NAO pair, the R^2 values for all 12 various ENSO indices and for all three time series of global temperature reached 0.698, indicating that a large proportion, nearly 70%, of the medium-term annual variability of temperature is explained by the ENSO and AMO evolution. For ENSO and IPO TPI pairs, the R^2 values reached 0.612, while 0.632 for AMO and IPO TPI.

The joint consideration of a triplet: ENSO, IPO TPI, and AMO improved the overall performance a little bit, with R2 reaching 0.707

Our results on links between ocean-atmosphere oscillation and global temperature, for ENSO, IPO TPI and AMO, are robust across the various global temperature datasets stemming from three institutions. The notion of robustness can be extended for 12 various definitions of ENSO indices, for all of which meaningful correlations with residuals of global temperature were found.

This communication demonstrates clear and easily understandable links between residuals of global temperature and ENSO, IPO and AMO indices of climate variability. Our approach follows the spirit of exploratory data analysis. We succeeded in reading the pattern that is present in the data and unveiled interesting links.

The simplicity of the methodology in our study is its major strong point. According to our knowledge, no one has followed a similar methodology. The variety of indices we studied, as well the combinations thereof in pairs and triplet, is another point of novelty of our study. Other authors had done studies on links to one oscillation index, quite a long time ago, so that the studied records terminated one, two or three decades earlier than ours (extending until 2019). This update to the present time is an additional noteworthy contribution, particularly because it includes interesting periods such as the “hiatus” (Cowtan & Way, 2014; England et al., 2014; Karl et al., 2015) and the post-hiatus recent years, the warmest on record. We have linked the dots that are readily available, in a transparent and reproducible way, locating general behaviours applicable on the entire record, rather than specific patterns of subperiods (e.g. the “hiatus”). In our opinion, our results are persuading, easy to understand and to reproduce, and of relevance and interest to the broad scientific community. A final remarkable feature of our study is that we let the data speak for themselves, without introducing a subjective distortion by data transformation, let alone by using models. In our opinion, this has augmented the power of our results.

Implicitly, the study points to a research direction that recognizes the importance of the data over models. The exploration of the data can identify patterns that should then be used as benchmarks for models, in the sense that the models should mimic or reproduce those patterns. Deterministic models would be useful to explain those patterns, possibly providing a causation frame, but before explanation a model should be able to reproduce them. Even for establishing a causation frame, the results of this study would be useful. For example, the time lags identified between temperature and the ocean-atmosphere oscillations provide a dominant direction of causality. Once a deterministic model proves consistent with the patterns identified by the exploratory data analysis, it could possibly be used operationally, e.g. for future prediction. But even in the absence of such a deterministic model, the high coefficients of determination that have been identified could possibly enable other types of prediction, such as stochastic or computational intelligence methods. These questions would be addressed in future research.

Acknowledgements

ZWK and IP wish to acknowledge financial support from the project: “Interpretation of Change in Flood-Related Indices based on Climate Variability” (FloVar) funded by the National Science Centre of Poland (project number 2017/27/B/ST10/00924). The co-authors would also like to acknowledge the data sources, as mentioned in the section on Data availability. DK is thankful to ZWK and IP for the invitation to contribute to this research, even though he did not participate in the project and he did not receive any financial support. The co-authors kindly acknowledge useful and constructive reviews of two anonymous reviewers that helped us in improving the paper and presentation of the material.

Author contributions. ZWK conceived the study and drafted the skeleton of the paper. IP and DK modified and enriched the ideas of ZWK. IP and DK conducted the calculations. All three co-authors discussed the results and edited the manuscript.

Competing interests. There are no competing interests.

Data availability. Data on global temperature and on ENSO indices, available in open access sources, were retrieved from sites listed in tables S1 and S2, respectively and in the links shown in the text.

References

Brohan, P., Kennedy, J. J., Harris, I., Tett, S. F. B. and Jones, P. D. (2006) Uncertainty estimates in regional and global observed temperature changes: A new dataset from 1850. *J. Geophys. Res.* 111, D12106. doi:10.1029/2005JD006548

Cohn, T. A., Lins, H. F. (2005) Nature's style: Naturally trendy. *Geophys. Res. Lett.* 32, L23402, doi:10.1029/2005GL024476

Cowtan, K., Way, R. G. (2014) Coverage bias in the HadCRUT4 temperature series and its impact on recent temperature trends. *Quarterly Journal of the Royal Meteorological Society* 140(683): 1935-1944. https://doi.org/10.1002/qj.2297

England, M. H., Mcgregor, S., Spence, P., Meehl, G. A., Timmermann, A., Cai, W., Gupta, A.S., McPhaden, M.J., Purich, A., Santoso, A. (2014) Recent intensification of wind-driven circulation in the Pacific and the ongoing warming hiatus. *Nature Climate Change* 4(3): 222-227. https://doi.org/10.1038/nclimate2106

Folland, C. K., Parker, D. E., Kates, F. E. (1984) Worldwide marine temperature fluctuations 1856-1981. *Nature* 310(5979): 670-673.

Frajka-Williams, E., Beaulieu, C., Duchez, A. (2017) Emerging negative Atlantic Multidecadal Oscillation index in spite of warm subtropics. *Scientific Reports* 7:11224. doi: 10.1038/s41598-017-11046-x

Hamed, K. H. (2008) Trend detection in hydrologic data: The Mann-Kendall trend test under the scaling hypothesis. *Journal of Hydrology* 349(3–4): 350-363. doi:10.1016/j.jhydrol.2007.11.009

Harris, I., Jones, P. D., Osborn, T. J., Lister, D. H. (2014) Updated high-resolution grids of monthly climatic observations – the CRU TS3.10 Dataset. *International Journal of Climatology* 34(3): 623-642.

Henley, B. J., King, A. D. (2017) Trajectories toward the 1.5°C Paris target: Modulation by the Interdecadal Pacific Oscillation. *Geophysical Research Letters* 44(9), 4256-4262. https://doi.org/10.1002/2017GL073480

IPCC (Intergovernmental Panel on Climate Change) (1990) *Climate Change: The IPCC Scientific Assessment* (edited by Houghton, J. T., Jenkins, G. J. and Ephraums, J. J.). Report prepared for Intergovernmental Panel on Climate Change by Working Group I. Cambridge University Press, Cambridge, U.K., New York, NY, USA and Melbourne, Australia.

IPCC (1995) *Climate Change 1995 - The Science of Climate Change* (edited by Houghton, J. T., Meira Filho, L. G., Callander, B. A., Harris, N., Kattenberg A. and Maskell, K.). Contribution of Working Group I to the Second Assessment Report of the Intergovernmental Panel on Climate Change. Cambridge University Press, Cambridge, UK and New York, NY, USA.

IPCC (2001) *Climate Change 2001: The Scientific Basis* (edited by Houghton, J. T., Ding, Y., Griggs, D. J., Nouger, M., van der Linden, P. J., Dai, X., Maskell, K. and Johnson, C. A.). Contribution of the Working Group I to the Third Assessment Report of the Intergovernmental Panel on Climate Change, Cambridge University Press, Cambridge, UK and New York, NY, USA.

IPCC (2007) *Climate Change 2007: The Physical Science Basis* (edited by Solomon, S., Qin, D., Manning, M., Chen, Z., Marquis, M., Averyt, K.B., Tignor, M.and Miller, H. L.) Contribution of Working Group I to the Fourth Assessment Report of the Intergovernmental Panel on Climate Change. Cambridge University Press, Cambridge, UK and New York, NY, USA.

IPCC (2013) *Climate Change 2013: The Physical Science Basis* (edited by Stocker, T. F., Qin, D., Plattner, G.-K., Tignor, M., Allen, S. K., Boschung, J., Nauels, A., Xia, Y., Bex, V. and Midgley P. M.). Contribution of Working Group I to the Fifth Assessment Report of the Intergovernmental Panel on Climate Change Cambridge University Press, Cambridge, UK and New York, NY, USA.

Kaplan, A. (2011) Patterns and indices of climate variability. In: State of the Climate in 2010. *Bull. Amer. Meteor. Soc*. 92(6): S20-S26.

Karl, T. R., Arguez, A., Huang, B., Lawrimore, J. H., McMahon, J. R., Menne, M. J., Peterson, T.C., Vose, R.S. and Zhang, H.-M. (2015) Possible artifacts of data biases in the recent global surface warming hiatus. *Science* 348(6242): 1469-72. https://doi.org/10.1126/science.aaa5632

Kerr, R. C. (2000) A North Atlantic climate pacemaker for the centuries. *Science* 288(5473): 1984-1985.

Koutsoyiannis, D. (2003) Climate change, the Hurst phenomenon, and hydrological statistics. *Hydrological Sciences Journal* 48(1): 3–24, doi:10.1623/hysj.48.1.3.43481

Koutsoyiannis, D., Montanari, A. (2007) Statistical analysis of hydroclimatic time series: Uncertainty and insights. *Water Resources Research*, 43(5): W05429, doi:10.1029/2006WR005592

Kundzewicz, Z. W., Matczak, P., Otto, I. M., Otto, P. E. (2020) From "atmosfear" to climate action. *Environmental Science and Policy* 105(2020): 75-83.

Kundzewicz, Z. W., Painter, J., Kundzewicz, W. J. (2019a) Climate change in the media: Poland's exceptionalism. *Environmental Communication* 13(3): 366-380. https://doi.org/10.1080/17524032.2017.1394890

Kundzewicz, Z.W., Szwed, M., Pińskwar, I. (2019b) Climate variability and floods-A global review. *Water* 11(7): 1399.

Mann, M. E., Park, J. (1994) Global modes of surface temperature variability on interannual to century time scales. *J. Geophys. Res.* 99, 25819-25833.

Mann, M. E., Steinman, B. A., Miller, S. K. (2014) On forced temperature changes, internal variability, and the AMO. *Geophysical Research Letters* 41(9), 3211-3219. https://doi.org/10.1002/2014GL059233@10.1002

Mason, B. G., Pyle, D. M., Oppenheimer, C. (2004) The size and frequency of the largest explosive eruptions on Earth. *Bull. Volcanol.* 66(8): 735-748. doi: 10.1007/s00445-004-0355-9

McPhaden, M. J., Zebiak, S. E., Glantz, M. H. (2006) ENSO as an Integrating Concept in Earth Science. *Science* 314: 1740-1745.

Nagy, M., Petrovay, K., Erdélyi, R. (2017) The Atlanto- Pacific multidecade oscillation and its imprint on the global temperature record. *Climate Dynamics* 48:1883-1891.

Newhall, C. G., Self, S. (1982) The volcanic explosivity index (VEI) an estimate of explosive magnitude for historical volcanism. *J. Geophys. Res.* 87(C2): 1231-1238. doi: 10.1029/JC087iC02p01231

Norel, M., Kałczyński, M., Pińskwar, I., Krawiec, K., Kundzewicz, Z. W. (2020) Climate variability indices – a guided tour. *Earth System Science Data* (submitted, in review).

Power, S., Casey, T., Folland, C., Colman, A., Mehta, V. (1999) Inter-decadal modulation of the impact of ENSO on Australia. *Climate Dynamics* 15(5), 319-324. https://doi.org/10.1007/s003820050284

Rayner, N. A. Brohan, P., Parker, D. E., Folland, C. K., Kennedy, J. J., Vanicek, M., Ansell, T. J., Tett S. F. B. (2006) Improved analyses of changes and uncertainties in sea surface temperature measured in situ since the mid-nineteenth century: The HadSST2 data set. *Journal of Climate* 19: 446-469.

Schlesinger, M. E., Ramankutty, N. (1994) An oscillation in the global climate system of period 65-70 years. *Nature* 367(6465): 723-726.

Schlesinger, M. E., Ramankutty, N. (1995) Is the recently reported 65- to 70-year surface-temperature oscillation the result of climatic noise? *Journal of Geophysical Research* 100**:** 13767-13774.

Stanisławska, K., Krawiec, K., Kundzewicz, Z. W. (2012) Modeling global temperature changes with genetic programming. *Computers & Mathematics with Applications* 64: 3717-3728.

Stanisławska, K., Kundzewicz, Z. W., Krawiec, K. (2013) Hindcasting global temperature by evolutionary computation. *Acta Geophysica* 61(3): 732-751.

Thompson, D. W. J., Wallace, J. M., Jones, P. D., Kennedy, J. J. (2009) Identifying signatures of natural climate variability in time series of global-mean surface temperature: Methodology and insights. *Journal of Climate* 22: 6120-6141.

Tourre, Y. M., White, W. B. (1995) ENSO signals in global upper-ocean temperature. *Journal of Physical Oceanography* 25: 1317-1322.

Trenberth, K. E., Fasullo, J. T., Kiehl, J. (2009) Earth's global energy budget. *Bull. Am. Meteorol. Soc***.** 90: 311-323.

Tsonis, A. A., Elsner, J. B., Hunt, A. G., Jagger, T. H. (2005) Unfolding the relation between global temperature and ENSO. *Geophysical Research Letters* 32: L09701.

van der Werf, G. R., Dolman, A. J. (2014) Impact of the Atlantic Multidecadal Oscillation (AMO) on deriving anthropogenic warming rates from the instrumental temperature record. *Earth System Dynamics* 5: 375-382.

Yulaeva, E., Wallace, J. M. (1994) The signature of ENSO in global temperature and precipitation fields derived from the microwave sounding unit. *Journal of Climate* 7: 1719-1736.

Table 1. Change in global mean temperature in °C / 100 years, and values of coefficient of determination (R^2) between the time [in years] and time series of annual global mean temperature anomalies, for shifted 30-year intervals and for the whole examined interval.

Time interval	Source for global mean temperature anomalies (land and ocean)					
	NASA		NOAA		CRU	
	Change (°C / 100 years)	R^2	Change (°C / 100 years)	R^2	Change (°C / 100 years)	R^2
1880-1909	-0.58	0.1933	-0.64	0.2449	-0.52	0.1769
1890-1919	-0.45	0.1159	-0.27	0.0429	-0.03	0.0007
1900-1929	0.23	0.0330	0.36	0.0795	0.71	0.2443
1910-1939	1.00	0.5275	1.00	0.5339	1.27	0.6354
1920-1949	1.20	0.5088	1.25	0.4963	1.06	0.6129
1930-1959	0.32	0.0550	0.35	0.0531	0.28	0.0620
1940-1969	-0.42	0.1196	-0.42	0.0964	-0.25	0.055
1950-1979	0.44	0.1472	0.44	0.1234	-0.04	0.0009
1960-1989	1.27	0.5592	1.20	0.5157	0.69	0.2471
1970-1999	1.69	0.6952	1.69	0.6984	1.71	0.6856
1980-2009	1.68	0.7215	1.55	0.7165	1.78	0.7589
1990-2019	2.10	0.8085	1.98	0.7859	1.72	0.7373
Whole available period	0.74	0.7456	0.74	0.7663	0.68	0.7748

Table 2. Highest values of coefficient of determination (R^2) between time series of residuals from 5-year running mean of temperature and of various ENSO indices. Temperature data stem from three sources: NASA; NOAA, CRU. The highest value of R^2 are marked in bold.

ENSO index residuals from 5-year running mean	Source of data for temperature anomalies					
	NASA		NOAA		CRU	
	12-month moving average	R^2	12-month moving average	R^2	12-month moving average	R^2
SOI CRU	Aug-Jul	0.400	Sep-Aug	0.439	Sep-Aug	0.419
SOI NOAA	Jul-Jun	0.468	Sep-Aug	0.536	Sep-Aug	0.566
SOI AU	Sep-Aug	0.410	Sep-Aug	0.449	Sep-Aug	0.433
Equatorial SOI	Jul-Jun	0.507	Aug-Jul	0.574	Aug-Jul	**0.590**
Equatorial SOI Indonesia	Jul-Jun	0.506	Jul-Jun	**0.575**	Jul-Jun	0.583
Equatorial SOI Eastern Pacific	Jul-Jun	0.426	Aug-Jul	0.478	Sep-Aug	0.493
Niño 1.2	Jul-Jun	0.425	Jul-Jun	0.454	Jul-Jun	0.464
Niño 3.4	Sep-Aug	0.507	Oct-Sep	0.546	Sep-Aug	0.532
Niño 3	Aug-Jul	**0.509**	Sep-Aug	0.553	Sep-Aug	0.541
Niño 4	Oct-Sep	0.479	Oct-Sep	0.511	Oct-Sep	0.504
EMI	Oct-Sep	0.159	Oct-Sep	0.153	Oct-Sep	0.160
ONI NOAA	JFM	0.409	FMA	0.478	FMA	0.498

Table 3. Highest values of R^2 between time series of residuals from 5-year running mean of temperature (land and ocean), of particular ENSO indices (as indicated) and of AMO index (12-month average: Jan-Dec). Temperature data stem from three sources: NASA; NOAA, CRU. The highest value of R^2 are marked in bold.

ENSO index residuals from 5-year running mean	Source of data for temperature anomalies					
	NASA		NOAA		CRU	
	12-month moving average	R^2	12-month moving average	R^2	12-month moving average	R^2
SOI CRU	Sep-Aug	0.534	Nov-Oct	0.597	Oct-Sep	0.563
SOI NOAA	Dec-Nov	**0.607**	Dec-Nov	**0.697**	Dec-Nov	**0.698**
SOI AU	Sep-Aug	0.536	Nov-Oct	0.598	Oct-Sep	0.565
Equatorial SOI	Sep-Aug	0.575	Nov-Oct	0.664	Nov-Oct	0.660
Equatorial SOI Indonesia	Jul-Jun	0.578	Jan-Dec	0.688	Dec-Nov	0.668
Equatorial SOI Eastern Pacific	Sep-Aug	0.557	Nov-Oct	0.628	Nov-Oct	0.617
Niño 1.2	Aug-Jul	0.515	Aug-Jul	0.571	Aug-Jul	0.557
Niño 3.4	Oct-Sep	0.580	Nov-Oct	0.652	Nov-Oct	0.611
Niño 3	Sep-Aug	0.576	Oct-Sep	0.643	Sep-Aug	0.611
Niño 4	Nov-Oct	0.581	Nov-Oct	0.642	Nov-Oct	0.613
EMI	Jan-Dec	0.454	Jan-Dec	0.498	Jan-Dec	0.469
ONI NOAA	AMJ	0.572	AMJ	0.649	AMJ	0.637

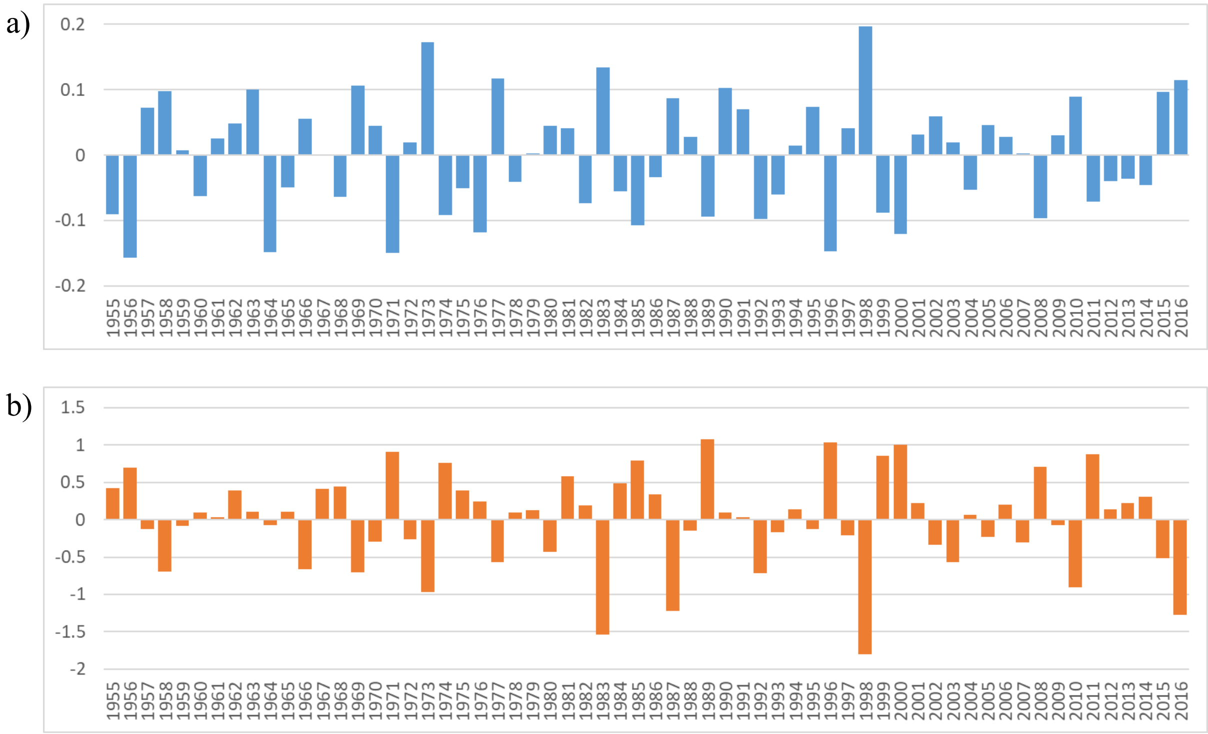

Figure 1. Residuals from 5-year running mean of (a) temperature (CRU) [in ^{o}C] and (b) Equatorial SOI index characterizing ENSO (Aug-Jul).

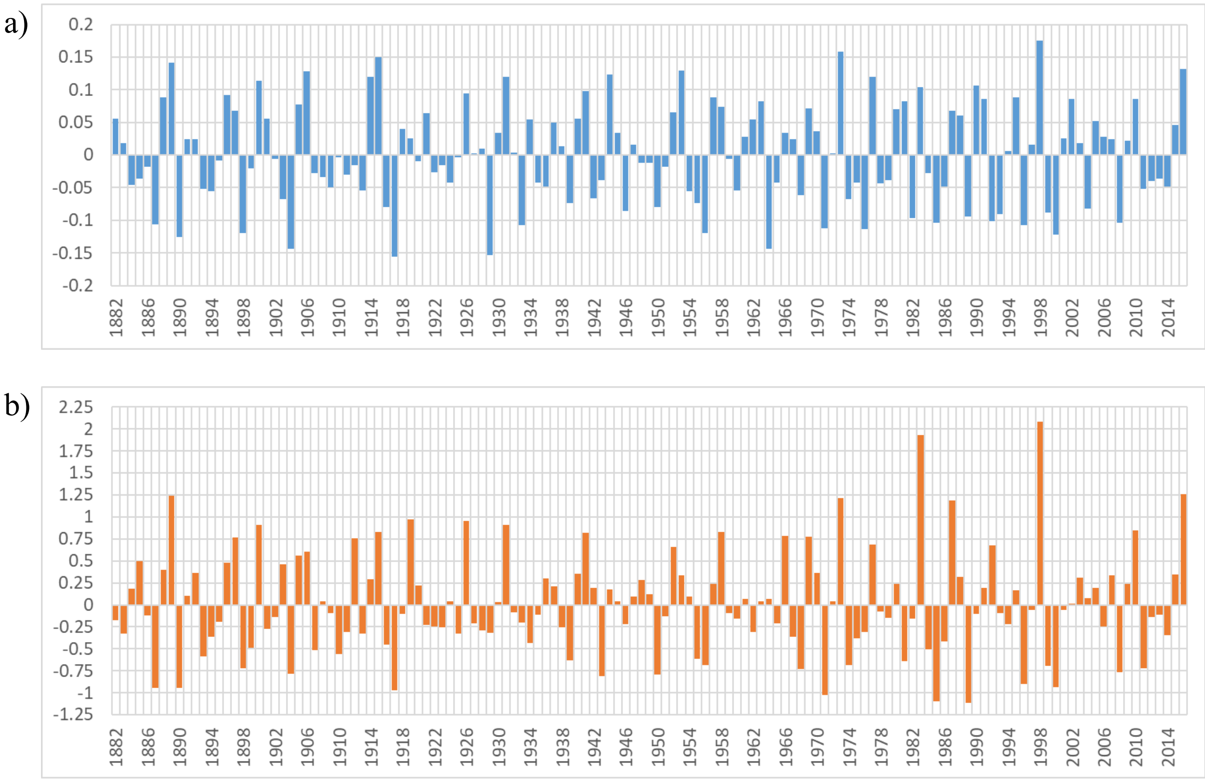

Figure 2. Residuals from 5-year running mean of temperature anomalies (NASA) [in °C] (a) and residuals from 5-year running mean of Niño 3 index (Aug-Jul) (b).

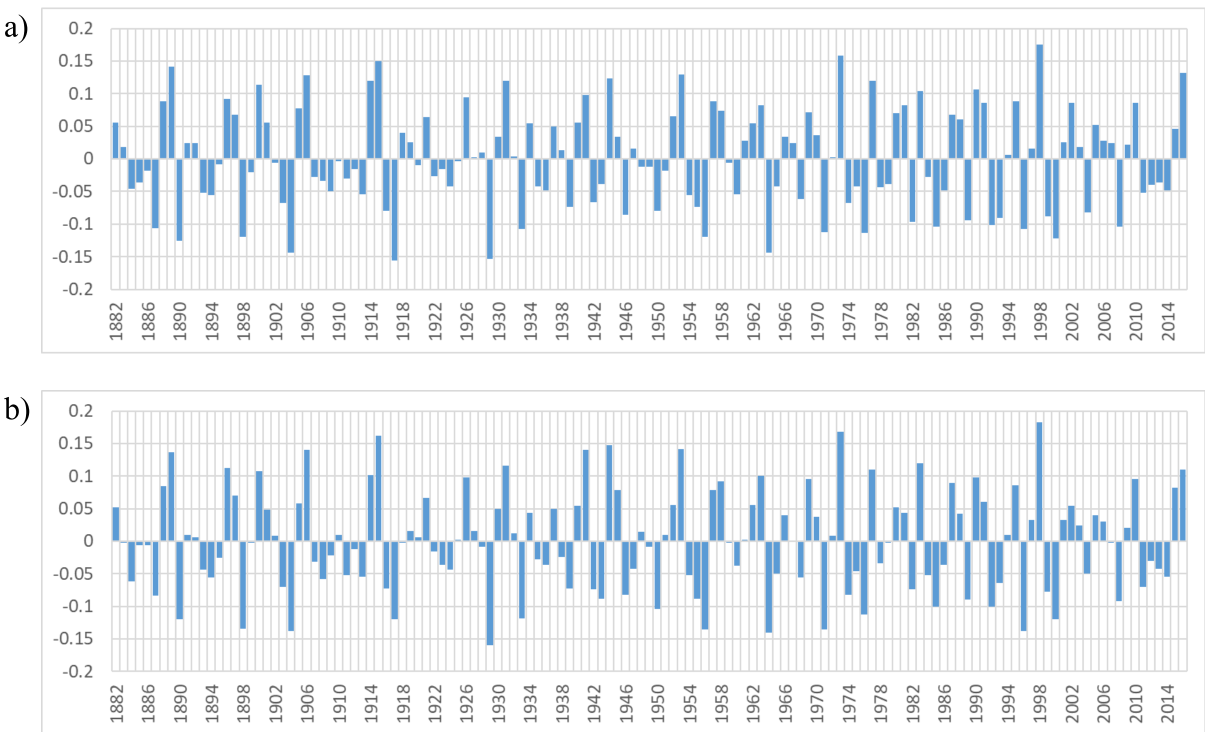

c)

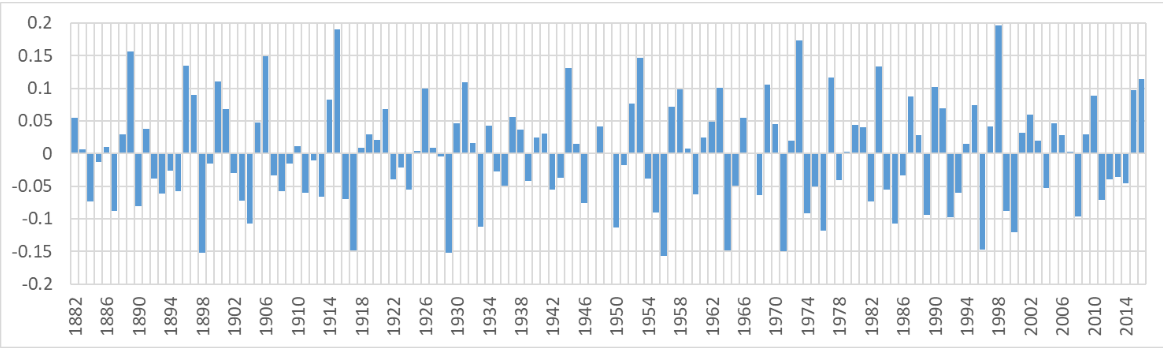

d)

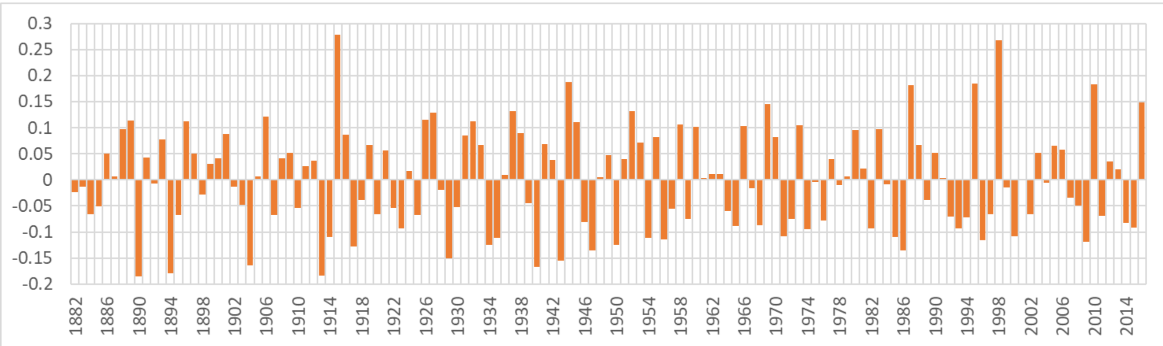

Figure 3. Residuals from 5-year running mean of global temperature anomalies, after NASA (a), NOAA (b), and CRU (c) and annual mean (Jan-Dec) of residuals from 5-year running mean values of the AMO index (d).